

Unraveling the Pathogenesis of Crimean-Congo Hemorrhagic Fever: A Novel Approach via Non-Targeted Metabolomics by NMR Spectroscopy

*Oktay Göcenler^{1,#}, Kerem Kahraman^{1,#}, Derya Yapar², Yaren Kahraman¹, Cengizhan Büyükdağ¹,
Gülen Esken³, Serena Ozabrahamyan⁴, Tayfun Barlas³, Yüksel Karadağ², Aysel Kocagül
Çelikbaş², Füsun Can^{3,5}, Nurcan Baykam², Mert Kuşkucu^{3,6}, Önder Ergönül^{3,6,*}, Çağdaş Dağ^{1,3,*}*

¹Nanofabrication and Nanocharacterization Center for Scientific and Technological Advanced Research (n²STAR), Koç University, İstanbul, Türkiye

²Department of Infectious Diseases and Clinical Microbiology, Çorum Erol Olçok Training and Research Hospital, Çorum, Türkiye

³Koç University Isbank Center for Infectious Diseases (KUISCID), Koc University, İstanbul, Türkiye

⁴The Ohio State University Wexner Medical Center, Columbus, USA

⁵Koç University School of Medicine, Department of Medical Microbiology, İstanbul, Türkiye

⁶Koç University School of Medicine, Department of Clinical Microbiology and Infectious Diseases, İstanbul, Türkiye

*Corresponding author: cdag@ku.edu.tr, oergonul@ku.edu.tr

#equal contribution

SUMMARY

The application of metabolomics for studying modifications in host metabolism due to viral infections has proven to be a game-changing approach. Prior to our study, only one other 'omics' study has been carried out that investigates the interplay between the host and CCHFV and its subsequent pathogenesis. We employed NMR spectroscopy, given its advantages in terms of reproducibility, minimal sample preparation, and capability to analyze complex biofluids. Our methodology builds upon the proven success of metabolomics in the research of other viral hemorrhagic fevers such as Ebola, Marburg, and Dengue. Our research underlines the critical role of SAH, a metabolite involved in numerous biochemical reactions. We provide new insights into the metabolic alterations occurring in CCHF patients. These alterations not only shed light on the disease's pathogenesis but also pave the way for potential biomarkers and therapeutic targets. Among all the metabolites detected, S-Adenosyl-L-homocysteine and Carnosine stood out as the most prevalent, warranting further exploration of their roles in CCHFV pathogenesis and their potential as therapeutic targets.

1. Introduction

Crimean-Congo Hemorrhagic Fever (CCHF) is a severe viral infection with substantial implications for public health in a wide range of countries in Asia, Africa, Southern Europe and the Middle East. CCHF is caused by CCHF virus (CCHFV) belonging to the genus of Orthonairovirus, and the family of Nairoviridae being one of deadliest viruses of its kind with reported mortality rate of 3-30% (1). CCHFV is transmitted to humans through tick bites of infected ticks, contact with blood or tissues of infected livestock, or contact with infected patients (2). The exact course of pathogenesis of CCHF is not clearly known however it is divided into four phases: incubation, pre-haemorrhagic, haemorrhagic and convalescence (2, 3). CCHF is classified as a severe hemorrhagic fever with a short incubation period of 1-3 days although longer incubation periods have been documented (3, 4). The onset of infection is often sudden and includes symptoms, fever, diarrhea, vomiting, nausea, myalgia, back and abdominal pain followed by an hemorrhagic phase where severe bruises, uncontrollable bleeding at the body orifices are observed and in severe cases, deterioration of kidneys, liver and lungs (5). Deaths associated with the infection mostly occur between 5-14 days from the start of the viremic phase (6, 7). In terms of treatment, early hospitalizations and early administration of therapeutics are shown to reduce both severity and mortality of CCHF (8). Hence, lack of early detection of CCHF is one of the leading factors causing the particular high mortality rate of CCHF.

There are several challenges of diagnosing CCHF infection particularly before the hemorrhagic phase of the infection and patients who are not suspected of being bitten by infected ticks or contacted with infected livestock. CCHF is relatively rare in certain areas, so healthcare providers may not consider CCHF as a possible diagnosis at first. Likewise, there are

documented cases of difficulties diagnosing CCHF, both because of the latter but also the absence of a universally applicable diagnostic kit for surveillance and diagnosis of all CCHFV strains (9). Standard blood tests such as hemogram, biochemical analysis and physical examination at the beginning of hospitalization is applied on all patients who are suspected to be infected with CCHF although the results are often relevant for short term prognostic factors as biochemical values change often quickly. More comprehensive tests such as viral antigen and nucleic acid amplification tests are used as standard diagnostic methods (10). The initial symptoms of CCHF, such as fever, headache, and muscle aches, are rather non-specific hence diagnosing CCHF early by differential diagnosis can be difficult. (3,6) Biomarkers, essentially biomolecules, provide a measure of specific diseases or their stages due to their varying concentrations. They are instrumental in diagnosing and monitoring the progression of viral infections. The associated changes in their levels, often indicative of the disease, are typically attributed to the host's immune reaction and the disturbance of key biochemical routes in reaction to the infectious process. In this sense, omics studies and biomarkers could be used for both analysis and diagnosis of CCHF and for characterizing better treatment strategies of hospitalized patients swiftly is crucial to pinpoint optimal treatment strategies for treating CCHF (11).

So far there is only one omics study which investigates host-viral response and pathogenesis of CCHF utilizing transcriptomics and proteomics methods (12). Led by this gap in the literature, we conducted a nationwide analysis of metabolomes of patients hospitalized due to CCHF. Turkey has over 10,000 cases of CCHF with an average fatality rate of 5%, making it a critical public health concern affecting people living in rural areas as ticks are widespread in these regions (13). In our present investigation, we employed Nuclear Magnetic Resonance (NMR) spectroscopy exploratory metabolomics to investigate the overall temporal variations in plasma

metabolites during a seasonal outbreak of CCHF infection. We employed PLS-DA statistical analysis of the blood serum metabolome of CCHF patients and categorized certain metabolomes linked to metabolic dysregulation caused by CCHF. Preliminary results from our study suggest that specific metabolic markers can be identified in the serum of CCHF patients pointing to metabolic dysregulation, which may allow for earlier diagnosis and more targeted treatment strategies. Additionally, being the first study to categorize alterations of patient metabolome during CCHF viremic phase may be valuable for efforts to develop therapeutics or targeted treatment strategies to reduce the severity and high mortality rate of CCHF.

2. Materials and methods

Monitoring of CCHF diagnosed patients and collection of the samples from the patients:

Patients who were diagnosed with CCHF were selected from Çorum Hitit University Hospital. The first sample collection was conducted in April 2022, and blood samples were collected daily using Ethylenediaminetetraacetic acid (EDTA) tubes. In current metabolomics studies, opinions regarding the appropriate determination of sample size can considerably vary. However, numerous statistical analyses have underscored that a substantial sample size, for achieving meaningful results, around 30 samples (14). In this study, serum specimens were procured from 29 patients (n=29) diagnosed with CCHFV infection, as well as from 10 healthy control group. CCHF patients also admitted to the hospital with an infection diagnosis were subclassified into two categories based on their blood test values and symptoms: moderate (n=24) and severe (n=5). Four blood serum samples from patients each consecutive day (n=116 samples) and a single sample from the control group (n=10 samples) was taken. These blood samples were then subjected to centrifugation for 5 minutes at 3000g to separate the sample into plasma, white blood cell, and red blood cell phases. The plasma phase was extracted and subjected to

metabolite extraction using multiple approaches: single methanol extraction, triple alcohol extraction, Methanol-chloroform, Acetone, Acetonitrile, and Ultrafiltration. Cold methanol-chloroform was chosen as the most effective extraction and used for extraction of all samples. Only the polar metabolites in the plasma were investigated, while proteins and apolar compounds were removed from the plasma samples. Overall in this study, we utilized a rigorous approach to sample collection, preparation, and analysis to investigate polar metabolites in the plasma of CCHF patients (15, 16, 17).

Ethical Statement: The study was approved by Koç University Ethics Committee and all the procedures performed in this study involving human participants were in accordance with the ethical standards of the institutional research committee ethical standards. A written informed consent was obtained from all patients.

NMR sample preparation: 4 mL ice-cold methanol-chloroform (1:1) mixture was added to 2 mL serum for methanol-chloroform extraction. The mixture was vortexed for 30 seconds and incubated for 10 minutes on ice. After incubation the mixture was centrifuged at 4500g at 4°C for 30 minutes. The methanol phase was collected and dried using a vacuum concentrator. The dried samples were dissolved in 550 μ L D₂O based NMR sample solution (50 mM PBS (pH 7.4), 20mM NaCl, 1 mM DSS) for standardized sample preparation.

NMR data collection, processing and statistical analysis: 500 MHz Bruker Ascend magnet with BBO paired resonance probe and Avance NEO console was used for NMR data collection. 1D NOESY-presat (noesygppr1d) pulse sequence was used for data collection. Each NMR data spectrum is composed of 4K screening and 32K complex data points. Spectrum widths were set to 9615.4 Hz. Bruker Topspin 4.2.0 software was used for NMR data processing. Data was

divided into 0.02 ppm data packages along with their normalization coefficients. The dataset, which comprises data packets with a resolution of 0.02 ppm, was analyzed using the MetaboAnalyst 5.0 online metabolomics statistical analysis software. Henceforth the data will be referred to as (Bin.x.xx [ppm]) data packets and the day of when sample was taken. All data points were normalized using the average centering normalization method. Following this normalization, the dataset underwent statistical analysis using Partial Least Squares Discriminant Analysis (PLS-DA). PLS-DA is a classification and discrimination technique based on the Partial Least Squares (PLS) regression method. This method is widely utilized to determine the differences between classes, particularly in high-dimensional and multivariate datasets. PLS-DA is a commonly employed method in analyzing complex biological systems, such as metabolomics studies. The VIP Projection variable importance score plot is a graph that is utilized to assess the outcomes of PLS-DA and determine the most significant variables in the analysis. VIP scores quantify the importance of each variable (e.g., metabolites) in classification and aid in identifying the most critical features. VIP scores are computed based on the contribution of each variable to the components (latent variables) in the PLS-DA model. The values begin at 1, and higher VIP scores indicate that the variable is more important for classification. Variables with VIP scores greater than 1 are generally deemed significant, although this threshold may vary in practice. The VIP score plot displays the VIP scores of the variables on the vertical axis, while the variables themselves or their indices are shown on the horizontal axis. This graph facilitates the identification of important variables visually and helps focus on the variables that require prioritization in the analysis. In the VIP score graph, the peaks at the relevant ppm values that make up the data packages (Bin.x.xx) have been examined in more detail and the metabolites to which they belong have been identified. For this operation,

NMR spectra have been reopened, and the metabolites to which the peak in the relevant ppm region belongs have been determined using the Chenomx software. It is thought that some peaks might belong to metabolites not found in the database, and the molecules these peaks belong to have not been identified. Further investigation and characterization may be required to fully understand these unidentified peaks and their role in the overall metabolic profile, ensuring that the final analysis provides an accurate reflection of the biological system under investigation.

Metabolomic pathway visualization: All metabolic pathways visualized using Metastate software Version BETA (<https://metastate.bio>) (Metastate Bio Inc.). Metastate algorithm employs the Kyoto Encyclopedia of Genes and Genomes (KEGG) database as its foundational input source. Software systematically retrieves details pertaining to biological pathways, chemical compounds, and molecular reactions of interest. Software curates and assembles a dynamic graphical representation of the data.

3. Results

The demographic characteristics of the participants in the study, includes 29 patients diagnosed with CCHF and 10 healthy individuals serving as controls. The mean age of the control group was 50.1 years, with an age range between 40 to 64 years, while the CCHF patient group had a slightly higher mean age of 50.5 years, though with a wider age range of 22 to 77 years. In total 126 blood samples were collected, their serum extracted by methanol extraction, and NMR samples were prepared for all samples. Following metabolite extraction, NMR analyses were conducted on the samples. Finally, a statistical analysis approach was applied. In the statistical analyses, all samples collected over a period of 4 days. All groups were subjected to statistical evaluation as moderate, severe, and control groups as described in materials and methods.

In PLS-DA analysis, a model is developed to include the primary components (latent variables) of the data. The first five components are considered important in classifying the data and explain the majority of the dataset. The matching score plots exhibit these first five components in two-dimensional graphs and compare each component with another (Figure 1a). Subsequently, the next step involved obtaining the Partial Least Squares Discriminant Analysis (PLS-DA) score plot, as shown in Figure 1b demonstrates a high discrimination between healthy and diseased individuals. PLS-DA effectively deals with highly dimensional data, highlighting the relevant variables responsible for the distinction, thereby providing a clear differentiation between health states based on the variation and correlation within the biomarker data. In order to examine the significant data packets responsible for this discrimination, the PLS-DA VIP Projection variable importance score plot is illustrated in Figure 1c. This technique, graphically demonstrated in Figure 1c, reveals the variables that have substantial influence on the discrimination. VIP scores signify the importance of each variable in the model, enabling us to identify and focus on the key biomarkers that are significantly altering between healthy and diseased states. This plot aids in the in-depth interpretation of the complex multivariate data and fosters a more nuanced understanding of the disease markers. Figure 1c showcases the top 15 variables that have the greatest impact on discrimination among these variables. As shown in Figure 1c, it is noticeable that several data packets exhibit low concentration values (blue) in the control group and gradually increase towards higher concentrations with the passage of time. Ultimately as depicted in Figure 1d, the listed compounds exhibited a notable increase in their concentration, as substantiated by increased signals from their corresponding data buckets. Using a statistical analysis approach consisting of three different groups. Samples taken on four consecutive days from the two patient groups were successfully differentiated from the control group. However,

no discernible distinction was observed between the moderate and severe groups. Overall these compounds were detected to be elevated compared to the control: SAH, GTP, Carnosine, maleate, 2-Deoxyuridine, IMP, AMP and NADP+.

As a secondary approach to data analysis, data collected on the day 1 and day 2 were used as severe patient and moderate patient groups to further investigate the metabolite profile of the patients during the initial stages of hospitalization. Subsequently, only samples obtained on day 1 and day 2 were categorized as diseased samples, and the blood samples obtained from healthy individuals were designated as the control group for statistical analysis (Fig 2). In addition to compounds detected in our initial analysis novel compounds with significant increase during day 1 and 2 detected that may have a more active role in the pathogenesis.

Finally, in a comprehensive metabonomic analysis of CCHF patients' blood serum, distinct patterns of metabolites were observed between the severe and moderate infection levels. Specifically, through the PLS-DA score plots and Variable Importance Score (VIP) projections detailed in Figure 3, notable variations in the metabolite profiles were discerned. In the case of severe CCHF infections, the compounds AMP, IMP, and NAAD were identified as present within the serum, whereas they were not as significantly detected in the samples from patients with moderate infection levels. Conversely, GTP was found to be significantly increased in the samples of patients with moderate CCHF infection levels, but not in those categorized as severe. Overall the results outlined in our final analysis reveal a marked metabolic variety between the moderate and severe CCHF infection levels which may indicate the critical pathways in CCHF pathogenesis.

4. Discussion

In this study we demonstrated our results of the first non-targeted CCHF metabolomics study to improve the current understanding of the pathogenesis of CCHF for diagnostic purposes and aid studies on development of potential therapies against CCHF. Our main findings revealed considerable increases in the levels of SAH, GTP, Carnosine, Maleate, 2-Deoxyuridine, IMP, AMP and NADP⁺ in the blood serum of CCHF patients, suggesting these metabolites could play crucial roles in the pathogenesis of CCHF and therefore, potentially serve as important biomarkers for early detection and monitoring of the disease progression.

Metabolomics has emerged as a pivotal approach for inspecting the modifications in host metabolism elicited by viral infections. Up until the present, only a single omics study has been conducted by MS that explores the interaction between the host and CCHFV and the ensuing pathogenesis (12). NMR and MS are the two commonly utilized methods used for metabolomics studies with each having certain strengths and weaknesses depending on their purpose of use. NMR spectroscopy offers better reproducibility, minimal sample preparation, and the ability to analyze complex biofluids, whereas MS has relatively higher sensitivity and better for targeted metabolomics studies. Although reproducibility and superior comparability of NMR spectra across different instruments and laboratories compared to MS makes it preferable for non-targeted metabolome analysis for diagnostic and prognostic analysis of several diseases (18). NMR spectroscopy in metabolomics is used in analysis of infection on host metabolism and its implications for the pathogenesis of viruses such as HIV (20), Dengue virus (DENV) (21), Chikungunya virus (22) Metabolomics analysis has been employed in the study of other viral hemorrhagic fevers, such as Ebola, Marburg, and Dengue, with promising results for early diagnosis and prognosis prediction (23). Our study demonstrates a new path by harnessing the

power of NMR metabolomics analysis to further decipher the intricate interplay between the host and CCHFV and to elucidate the mechanisms of CCHFV pathogenesis.

S-adenosyl homocysteine (SAH) is an intermediate metabolite, a precursor to homocysteine and adenosine(24). Moreover, SAH is the substrate of SAH hydrolase enzyme which is a crucial enzyme involved in the S-adenosylmethionine (SAM/AdoMet) regeneration cycle (Figure 4a) (25). This cycle is noteworthy in the context of CCHF patients, as evidenced by increased SAH levels from the beginning of hospitalization. Furthermore, a genomic study investigating the effect of Methylene tetrahydrofolate reductase (MTHFR) polymorphism showed that MTHFR polymorphism creates a predisposition to milder CCHF (26). MTHFR's primary role as an enzyme in folate metabolism extends to functions related to methylation as well. Thus, we hypothesized that alterations in methylation pathways during the viremic phase of CCHF may serve as valid indicators of prognosis in CCHF patients. Furthermore, SAM is understood to function as a primary methyl donor in various cellular methylation reactions, including those necessary for the 5' RNA capping process (27). Similar to the methylation process in Flaviviruses (28, 29), the Ebola virus' L protein has been found to exhibit methyltransferase activity, affecting co-transcriptional modifications at the cap structure and internal adenosine-2'-O-methylation (30). This additional complexity in RNA methylation within some viral families could provide a framework to consider the implications of SAM-related domains in replication complexes as potential drug targets.

GTP, AMP and inosine monophosphate (IMP) are nucleotides involved in purine metabolism, which play a vital role in energy metabolism (Figure 4b), and nucleic acid synthesis (31). Increase in the level of GTP and IMP are known indicators for infection of several viruses belonging to Orthornavirae kingdom (32). In fact, increase in purine compounds can be

attributed to infection of CCHFV considering known effective broad spectrum antivirals such as Ribavirin as a nucleotide analog targets the substrate-binding site of the IMPDH enzyme and prevents binding of IMP causing reduction of RNA synthesis in infected cells (33, 34) through down regulating GTP synthesis. Monitoring the levels of these metabolites may provide vital insights into the efficacy of antiviral treatments, especially nucleotide analogs like Ribavirin. Identifying shifts in GTP and IMP concentrations could be a good addition to therapeutic strategies for clinical trials, optimizing the use of antiviral agents that target purine metabolism, and thereby enhancing the response to CCHF infection. (35, 36) Carnosine (beta-alanyl-L-histidine) (Figure 4c) is a dipeptide with antioxidant, free radical scavenging; anti-glycation, and antiinflammatory properties which is predominantly found in skeletal muscle and in the brain (29). Increase in carnosine levels may reflect changes in the antioxidant defense system, reduction of muscle mass due to hospitalization and infection related cell death and as a possible anti-inflammatory response to the CCHFV infection. Carnosine is considered as a potential therapy for Zika and Dengue viruses, (37) and SARS-CoV-2 (38) as it showed significant reduction in viral replication and ease the symptoms of these diseases, however the effectiveness of carnosine as a therapeutic against CCHF requires further investigation. 2'-Deoxyuridine (2'-dU) is an intermediate in the synthesis of thymidylate (Figure 4d), which acts as a precursor for DNA synthesis and Edoxudine as an antiviral therapeutic. (39). Increase in the levels of 2-deoxyuridine can have significant implications for viral pathogenesis as 2'-dU variants such as BVDU is effective against Herpes simplex virus type 1 (HSV-1) and varicella-zoster virus (VZV) (40). Nevertheless 2'-dU is an antiviral of DNA viruses and used as an indicator to determine presence of viruses which have DNA as their genetic material (41). Presumably 2'-dU levels increased in the blood serum may indicate a dysregulation in the

pyrimidine and energy metabolism in accordance to our other findings which signal metabolic disruption of these pathways. Nicotinamide Adenine Dinucleotide Phosphate (NADP⁺), another key metabolite, serves as a crucial cofactor in various enzymatic reactions, primarily within the pentose phosphate pathway, where it facilitates the synthesis of NADPH, essential for fatty acid synthesis and the regeneration of reduced glutathione. Additionally, NADP⁺ plays a vital role in supporting the body's antioxidant defense system and is involved in the reduction-oxidation (redox) reactions. It is difficult to definitively pinpoint why NADP⁺ increases in CCHF patients, as the underlying cause could be multifaceted, encompassing a range of biological, metabolic, and external factors. Furthermore in relation to our other findings it is possible that elevation of NADP⁺ also overlaps with increase of GTP, IMP, and AMP which take part in energy metabolism and nucleotide synthesis, as a possible indication of a coordinated increase in use of energy and nucleic acid synthesis.. This is further supported by our final analysis between severe and moderate infection CCHF in Fig 3, considering AMP, IMP and NAAD levels increased more significantly in severe cases signaling increased activity in metabolic pathways including these compounds. Maleate (cis-butenedioic acid), a dicarboxylic acid, and trans-isomer of fumaric acid is a metabolite taking role in nicotinate and nicotinamide metabolism. (42) Previous studies on rats have demonstrated that the injection of sodium maleate can induce a generalized renal transport defect resembling Fanconi syndrome. Furthermore, maleate has been shown to reduce cellular levels of coenzyme A, inhibit the tricarboxylic acid cycle, lower ATP concentrations, and affect various enzymatic activities. Its impact even extends to the ultrastructure of kidney cells. The elevated presence of maleate in the blood serum of CCHF patients could signal underlying metabolic and cellular disruptions, warranting further investigation into its potential role and implications in the disease. (43,44)

Conclusion

In this study we conducted a nationwide analysis of blood serum metabolites of patients admitted to hospital due to CCHF. We employed NMR spectroscopy as a novel approach to characterize host viral response and pathogenesis of CCHFV. Among detected compounds, most prevalent of them were detected to be SAH and carnosine and notable increases in compounds relating to TCA cycle, nucleic acid synthesis and redox related coenzymes in the cell.

Author Contributions

Çağdaş Dağ: Conceptualization, Methodology, Supervision, Funding acquisition, Writing-Reviewing and Editing, Writing-Original draft preparation **Kerem Kahraman:** Investigation, Formal analysis, Visualization, Writing-Reviewing and Editing **Oktay Göcenler:** Investigation, Formal analysis, Writing-Original Draft, Visualization **Derya Yapar:** Investigation **Yaren Kahraman:** Investigation, Formal analysis **Cengizhan Büyükdağ:** Formal analysis, Writing-Original Draft **Gülen Esken:** Methodology, Investigation **Serena Ozabrahamyan:** Methodology, Investigation **Tayfun Barlas:** Investigation **Yüksel Karadağ:** Investigation **Aysel Kocagül Çelikbaş:** Investigation **Fusun Can:** Supervision, Investigation **Nurcan Baykam:** Supervision, Investigation **Mert Kuşucu:** Supervision, Writing-Reviewing and Editing **Önder Ergönül:** Supervision, Funding acquisition, Conceptualization, Methodology

ACKNOWLEDGMENT

CD acknowledges support from TÜBİTAK (Project No: 221S353). The authors acknowledge the use of the services and facilities of n²STAR-Koç University Nanofabrication and Nanocharacterization Center for Scientific and Technological Advanced Research. The authors gratefully acknowledge use of the services and facilities of the Koç University Is Bank Infectious Disease Center (KUIS-CID). We are also immensely grateful to Fırat Kahya, Boran Saruhan and Oğuzcan Ünver for constructive feedback and for their comments.

References

1. Belhadi, D., Baied, M. E., Mulier, G., Malvy, D., Mentré, F., & Laouénan, C. (2022). The number of cases, mortality and treatments of viral hemorrhagic fevers: A systematic review. *PLOS Neglected Tropical Diseases*, 16(10), e0010889. <https://doi.org/10.1371/journal.pntd.0010889>
2. Hoogstraal H. (1979). The epidemiology of tick-borne Crimean-Congo hemorrhagic fever in Asia, Europe, and Africa. *Journal of medical entomology*, 15(4), 307–417. <https://doi.org/10.1093/jmedent/15.4.307>
3. Swanepoel, R., Shepherd, A. J., Leman, P., Shepherd, S. P., McGillivray, G., Erasmus, M. J., Searle, L., & Gill, D. (1987). Epidemiologic and clinical features of Crimean-Congo hemorrhagic fever in Southern Africa. *American Journal of Tropical Medicine and Hygiene*, 36(1), 120–132. <https://doi.org/10.4269/ajtmh.1987.36.120>
4. Whitehouse, C. A. (2004). Crimean?Congo hemorrhagic fever. *Antiviral Research*, 64(3), 145–160. <https://doi.org/10.1016/j.antiviral.2004.08.001>
5. Elaldi, N., Bodur, H., Ascioğlu, S., Celikbas, A. K., Özkurt, Z., Vahaboglu, H., Leblebicioglu, H., Yilmaz, N., Engin, A., Şencan, M., Aydin, K., Dokmetas, I., Çevik, M. A., Dokuzoğuz, B., Tasyaran, M. A., Öztürk, R., Bakir, M., & Uzun, R. (2009). Efficacy of oral ribavirin treatment in Crimean-Congo haemorrhagic fever: A quasi-experimental study from Turkey. *Journal of Infection*, 58(3), 238–244. <https://doi.org/10.1016/j.jinf.2009.01.014>
6. Swanepoel, R., Gill, D. E., Shepherd, A. J., Leman, P. A., Mynhardt, J. H., & Harvey, S. (1989). The clinical pathology of Crimean-Congo hemorrhagic fever. *Reviews of infectious diseases*, 11 Suppl 4, S794–S800. https://doi.org/10.1093/clinids/11.supplement_4.s794
7. Ergonul, O., Tunçbilek, S., Baykam, N., Celikbas, A. K., & Dokuzoğuz, B. (2006). Evaluation of Serum Levels of Interleukin (IL)–6, IL-10, and Tumor Necrosis Factor– α in Patients with Crimean-Congo Hemorrhagic Fever. *The Journal of Infectious Diseases*, 193(7), 941–944. <https://doi.org/10.1086/500836>
8. Ergonul O. (2008). Treatment of Crimean-Congo hemorrhagic fever. *Antiviral research*, 78(1), 125–131. <https://doi.org/10.1016/j.antiviral.2007.11.002>
9. Almayahi, Z. K., Kindi, H. A., Jabri, I. H. S. H. A., Shaqsi, N. H. K. A., Hattali, N. A., Hattali, A. A., Quyoodhi, B. A., & Dhuhli, K. A. (2022). Challenges in Diagnosis of Crimean-Congo Hemorrhagic Fever. *Infectious Diseases in Clinical Practice*, 30(2). <https://doi.org/10.1097/ipc.0000000000001108>
10. Raabe V. N. (2020). Diagnostic Testing for Crimean-Congo Hemorrhagic Fever. *Journal of clinical microbiology*, 58(4), e01580-19. <https://doi.org/10.1128/JCM.01580-19>
11. Mayne, E. S., George, J. A., & Louw, S. (2023). Assessing Biomarkers in Viral Infection. *Advances in experimental medicine and biology*, 1412, 159–173. https://doi.org/10.1007/978-3-031-28012-2_8

12. Neogi, U., Elaldi, N., Appelberg, S., Ambikan, A. T., Kennedy, E. V., Dowall, S. D., Bagci, B., Gupta, S., Murillo, J. R., Akusjärvi, S. S., Monteil, V., Marko-Varga, G., Benfeitas, R., Banerjee, A. C., Weber, F., Hewson, R., & Mirazimi, A. (2022). Multi-omics insights into host-viral response and pathogenesis in Crimean-Congo hemorrhagic fever viruses for novel therapeutic target. *eLife*, 11. <https://doi.org/10.7554/elife.76071>
13. Ak, Ç., Ergönül, Ö. & Gönen, M. A prospective prediction tool for understanding Crimean–Congo haemorrhagic fever dynamics in Turkey. *Clin. Microbiol. Infect.* 26, 123-e1 (2020).
14. Nyamundanda, G., Gormley, I.C., Fan, Y. et al. MetSizeR: selecting the optimal sample size for metabolomic studies using an analysis based approach. *BMC Bioinformatics* 14, 338 (2013). <https://doi.org/10.1186/1471-2105-14-338>
15. Nagana Gowda, G. A., & Raftery, D. (2014). Quantitating metabolites in protein precipitated serum using NMR spectroscopy. *Analytical chemistry*, 86(11), 5433–5440. <https://doi.org/10.1021/ac5005103>
16. McHugh, R. K., Votaw, V. R., Sugarman, D. E., & Greenfield, S. F. (2018). Sex and gender differences in substance use disorders. *Clinical psychology review*, 66, 12–23. <https://doi.org/10.1016/j.cpr.2017.10.012>
17. Markley, J. L., Brüschweiler, R., Edison, A. S., Eghbalian, H. R., Powers, R., Raftery, D., & Wishart, D. S. (2017). The future of NMR-based metabolomics. *Current opinion in biotechnology*, 43, 34–40. <https://doi.org/10.1016/j.copbio.2016.08.001>
18. Emwas, A. M. (2015). The Strengths and Weaknesses of NMR Spectroscopy and Mass Spectrometry with Particular Focus on Metabolomics Research. In *Methods in molecular biology* (pp. 161–193). Springer Science+Business Media. https://doi.org/10.1007/978-1-4939-2377-9_13
19. Costa dos Santos Junior, G., Pereira, C. M., Kelly da Silva Fidalgo, T., & Valente, A. P. (2020). Saliva NMR-based metabolomics in the war against COVID-19. *Analytical chemistry*, 92(24), 15688-15692.
20. Munshi, S. U., Rewari, B. B., Bhavesh, N. S., & Jameel, S. (2013). Nuclear magnetic resonance based profiling of biofluids reveals metabolic dysregulation in HIV-infected persons and those on anti-retroviral therapy. *PloS one*, 8(5), e64298. <https://doi.org/10.1371/journal.pone.0064298>
21. El-Bacha, T., Struchiner, C. J., Cordeiro, M. T., Almeida, F. C. L., Marques, E. T. A., & Da Poian, A. T. (2016). ¹H Nuclear Magnetic Resonance Metabolomics of Plasma Unveils Liver Dysfunction in Dengue Patients. *Journal of Virology*, 90(16), 7429–7443. <https://doi.org/10.1128/jvi.00187-16>
22. Shrinet, J., Shastri, J. S., Gaiind, R., Bhavesh, N. S., & Sunil, S. (2016). Serum metabolomics analysis of patients with chikungunya and dengue mono/co-infections reveals distinct metabolite

signatures in the three disease conditions. *Scientific reports*, 6, 36833. <https://doi.org/10.1038/srep36833>

23. Fu, X., Wang, Z., Li, L., Dong, S., Li, Z., Zhenzuo, J., Wang, Y., & Shui, W. (2016b). Novel Chemical Ligands to Ebola Virus and Marburg Virus Nucleoproteins Identified by Combining Affinity Mass Spectrometry and Metabolomics Approaches. *Scientific Reports*, 6(1). <https://doi.org/10.1038/srep29680>

24. Wang, Z., Liang, H., Cao, H., Zhang, B., Li, J., Wang, W., Qin, S., Wang, Y., Xuan, L., Lai, L., & Shui, W. (2019). Efficient ligand discovery from natural herbs by integrating virtual screening, affinity mass spectrometry and targeted metabolomics. *Analyst*, 144(9), 2881–2890. <https://doi.org/10.1039/c8an02482k>

25. Kotb, M., Mudd, S. H., Mato, J. M., Geller, A. M., Kredich, N. M., Chou, J. Y., & Cantoni, G. L. (1997). Consensus nomenclature for the mammalian methionine adenosyltransferase genes and gene products. *Trends in Genetics*, 13(2), 51–52. doi:10.1016/s0168-9525(97)01013-5

26. Karakus, N., Duygu, F., Rustemoglu, A., & Yigit, S. (2022). Methylene-tetrahydrofolate reductase gene C677T and A1298C polymorphisms as a risk factor for Crimean-Congo hemorrhagic fever. *Nucleosides, Nucleotides & Nucleic Acids*, 41(9), 878–890. <https://doi.org/10.1080/15257770.2022.2085296>

27. Byszewska, M., Śmietański, M., Purta, E., & Bujnicki, J. M. (2014). RNA methyltransferases involved in 5' cap biosynthesis. *RNA Biology*, 11(12), 1597–1607. <https://doi.org/10.1080/15476286.2015.1004955>

28. Brecher, M., Chen, H. S., Liu, B., Banavali, N. K., Jones, S., Zhang, J., Li, Z., Kramer, L. D., & Li, H. (2015b). Novel Broad Spectrum Inhibitors Targeting the Flavivirus Methyltransferase. *PLOS ONE*, 10(6), e0130062. <https://doi.org/10.1371/journal.pone.0130062>

29. Babizhayev, M. A., Seguin, M. C., Gueyne, J., Evstigneeva, R. P., Ageyeva, E. A., & Zheltukhina, G. A. (1994). L-carnosine (beta-alanyl-L-histidine) and carbinine (beta-alanylhistamine) act as natural antioxidants with hydroxyl-radical-scavenging and lipid-peroxidase activities. *The Biochemical journal*, 304 (Pt 2)(Pt 2), 509–516. <https://doi.org/10.1042/bj3040509>

30. Valle, C., Martin, B., Ferron, F., Roig-Zamboni, V., Desmyter, A., Debart, F., Canard, B., Coutard, B., & Decroly, E. (2021). First insights into the structural features of Ebola virus methyltransferase activities. *Nucleic Acids Research*, 49(3), 1737–1748. <https://doi.org/10.1093/nar/gkaa1276>

31. Henderson, J., Lowe, J. K., & Barankiewicz, J. (1977). Purine and Pyrimidine Metabolism: Pathways, Pitfalls and Perturbations. In *Novartis Foundation Symposium* (pp. 3–21). Wiley. <https://doi.org/10.1002/9780470720301.ch2>

32. Tong, X., Smith, J. N., Bukreyeva, N., Koma, T., Manning, J. C., Kalkeri, R., Kwong, A. D., & Paessler, S. (2018). Merimepodib, an IMPDH inhibitor, suppresses replication of Zika virus and other emerging viral pathogens. *Antiviral Research*, 149, 34–40. <https://doi.org/10.1016/j.antiviral.2017.11.004>
33. Tchesnokov, E. P., Bailey-Elkin, B. A., Mark, B. L., & Götte, M. (2020). Independent inhibition of the polymerase and deubiquitinase activities of the Crimean-Congo Hemorrhagic Fever Virus full-length L-protein. *PLOS Neglected Tropical Diseases*, 14(6), e0008283. <https://doi.org/10.1371/journal.pntd.0008283>
34. Espy, N., Pérez-Sautu, U., De Arellano, E. R., Negrodo, A., Wiley, M. R., Bavari, S., Menéndez, M., Sánchez-Seco, M. P., & Palacios, G. (2018). Ribavirin Had Demonstrable Effects on the Crimean-Congo Hemorrhagic Fever Virus (CCHFV) Population and Load in a Patient With CCHF Infection. *The Journal of Infectious Diseases*, 217(12), 1952–1956. <https://doi.org/10.1093/infdis/jiy163>
35. Robins, R. K., Revankar, G. R., McKernan, P. A., Murray, B. K., Kirsi, J. J., & North, J. A. (1985). The importance of IMP dehydrogenase inhibition in the broad spectrum antiviral activity of ribavirin and selenazofurin. *Advances in Enzyme Regulation*, 24, 29–43. [https://doi.org/10.1016/0065-2571\(85\)90068-8](https://doi.org/10.1016/0065-2571(85)90068-8)
36. Leyssen, P., Balzarini, J., De Clercq, E., & Neyts, J. (2005). The Predominant Mechanism by Which Ribavirin Exerts Its Antiviral Activity In Vitro against Flaviviruses and Paramyxoviruses Is Mediated by Inhibition of IMP Dehydrogenase. *Journal of Virology*, 79(3), 1943–1947. <https://doi.org/10.1128/jvi.79.3.1943-1947.2005>
37. Rothan, H. A., Abdulrahman, A. Y., Khazali, A. S., Rashid, N. N., Chong, T. T., & Yusof, R. (2019). Carnosine exhibits significant antiviral activity against Dengue and Zika virus. *Journal of Peptide Science*, 25(8). <https://doi.org/10.1002/psc.3196>
38. Saadah, L. M., Deiab, G. I. A., Al-Balas, Q., & Basheti, I. A. (2020). Carnosine to Combat Novel Coronavirus (nCoV): Molecular Docking and Modeling to Cocrystallized Host Angiotensin-Converting Enzyme 2 (ACE2) and Viral Spike Protein. *Molecules*, 25(23), 5605. <https://doi.org/10.3390/molecules25235605>
39. Chon, J., Stover, P. J., & Field, M. S. (2017). Targeting nuclear thymidylate biosynthesis. *Molecular Aspects of Medicine*, 53, 48–56. <https://doi.org/10.1016/j.mam.2016.11.005>
40. De Clercq E. (2005). Potential clinical applications of the CXCR4 antagonist bicyclam AMD3100. *Mini reviews in medicinal chemistry*, 5(9), 805–824. <https://doi.org/10.2174/1389557054867075>
41. Yen, Y. C., Kong, L. X., Lee, L., Zhang, Y. Q., Li, F., Cai, B. J., & Gao, S. Y. (1985). Characteristics of Crimean-Congo hemorrhagic fever virus (Xinjiang strain) in China. *The American journal of tropical medicine and hygiene*, 34(6), 1179–1182

42. National Center for Biotechnology Information (2023). PubChem Compound Summary for CID 444266, Maleic Acid. Retrieved August 15, 2023 from <https://pubchem.ncbi.nlm.nih.gov/compound/Maleic-Acid>

43. Bergeron, M. G., Mayers, P., & Brown, D. T. (1996). Specific effect of maleate on an apical membrane glycoprotein (gp330) in proximal tubule of rat kidneys. *American Journal of Physiology-renal Physiology*, 271(4), F908–F916. <https://doi.org/10.1152/ajprenal.1996.271.4.f908>

44. Berliner, R. W., Kennedy, T. J., & Hilton, J. G. (1950). Effect of maleic acid on renal function. *Experimental Biology and Medicine*, 75(3), 791–794. <https://doi.org/10.3181/00379727-75-18344>

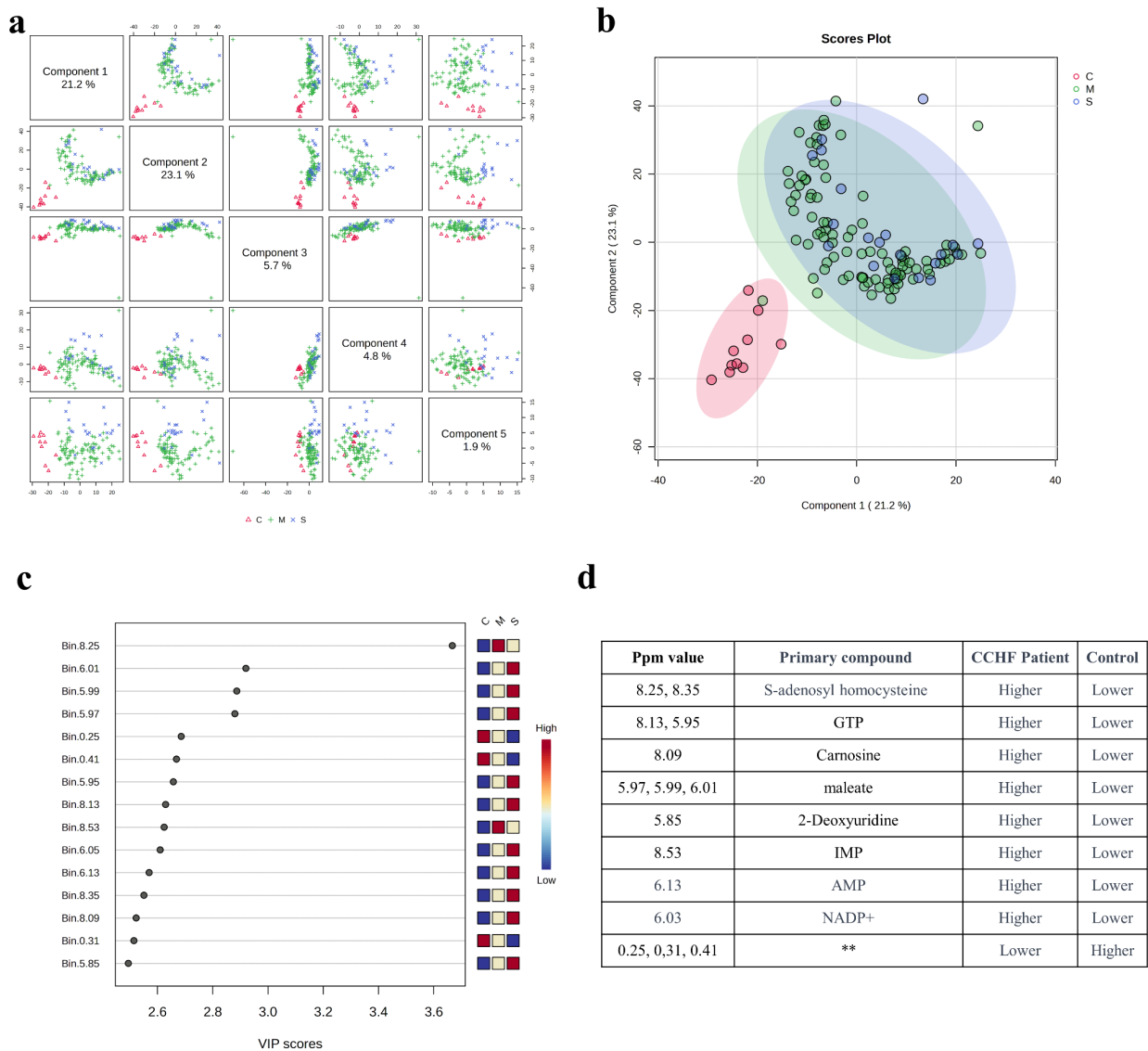


Figure 1: PLS-DA analysis of patient samples with severe and moderate infection level for four consecutive days with the control group (S:severe, M: moderate, C:Control) a. Matching score plots for the first five components of the PLS-DA analysis of all samples. b. partial Least Squares Discriminant Analysis score plot. c. Variable importance score plot in PLS-DA VIP Projection. d. corresponding compounds in detected increases on the spectra. Component 1: accuracy=0.817, ($R^2=0.246$, $Q^2=0.142$), component 2: accuracy=0.833, ($R^2=0.394$, $Q^2=0.210$), component 3: accuracy=0.809, ($R^2=0.545$, $Q^2=0.225$), component 4: accuracy=0.777, ($R^2=0.644$, $Q^2=0.250$), component 5: accuracy=0.769, ($R^2=0.782$, $Q^2=0.205$)

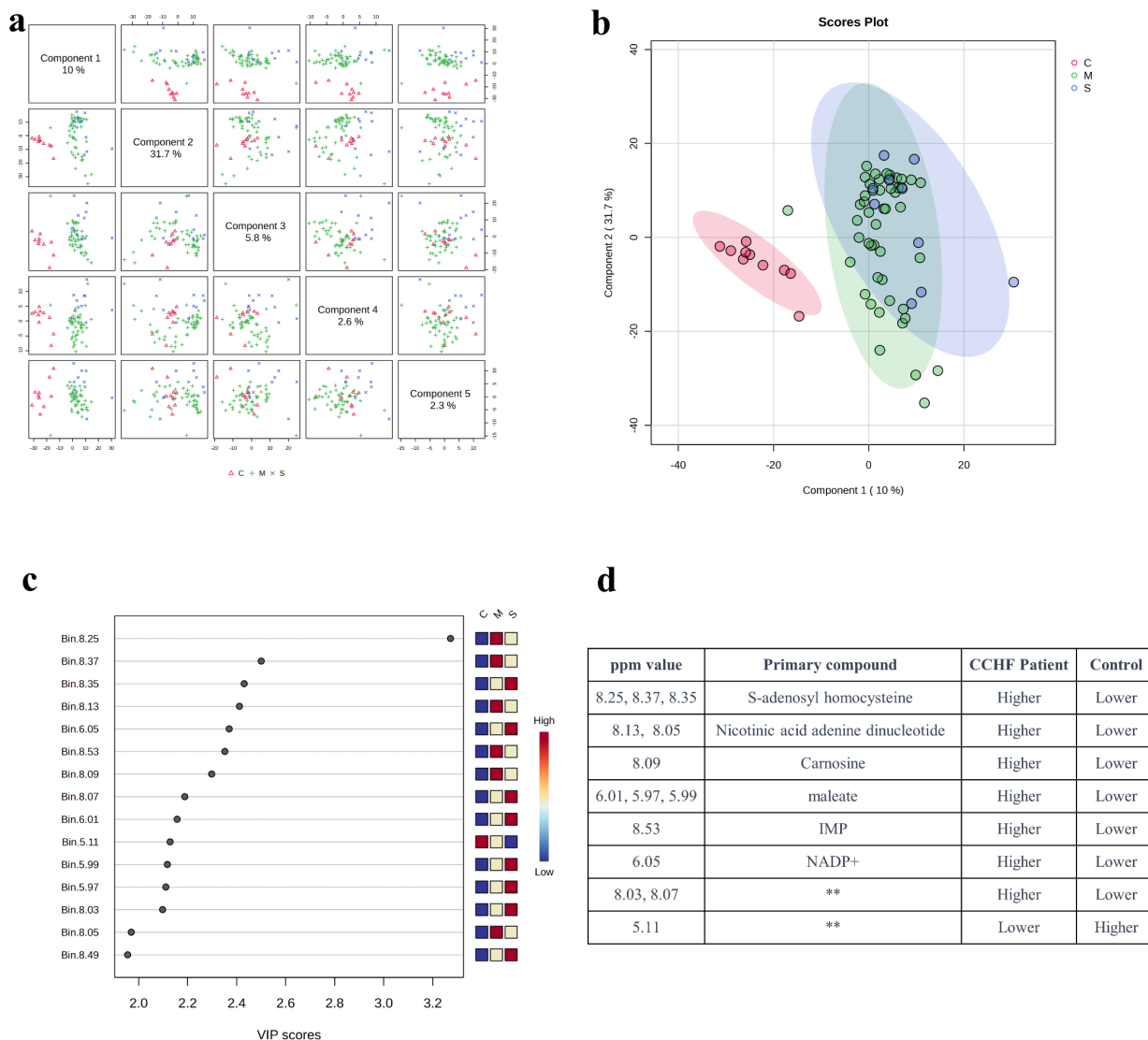


Figure 2: PLS-DA analysis of patient samples with severe and moderate infection level for first two days with the control group Matching score plots for the first five components of the PLS-DA analysis of samples from day 1 and day 2 as labeled mild (M), severe (S) and compared with the control group (C). b, partial Least Squares Discriminant Analysis score plot. c, Variable importance score plot in PLS-DA VIP Projection. d, corresponding compounds in detected increases on the spectra. Component 1: accuracy=0.0837, (R2=0.585, Q2=0.417), component 2: accuracy=0.821, (R2=0.627, Q2=0.433), component 3: accuracy=0.793, (R2=0.804, Q2=0.352)

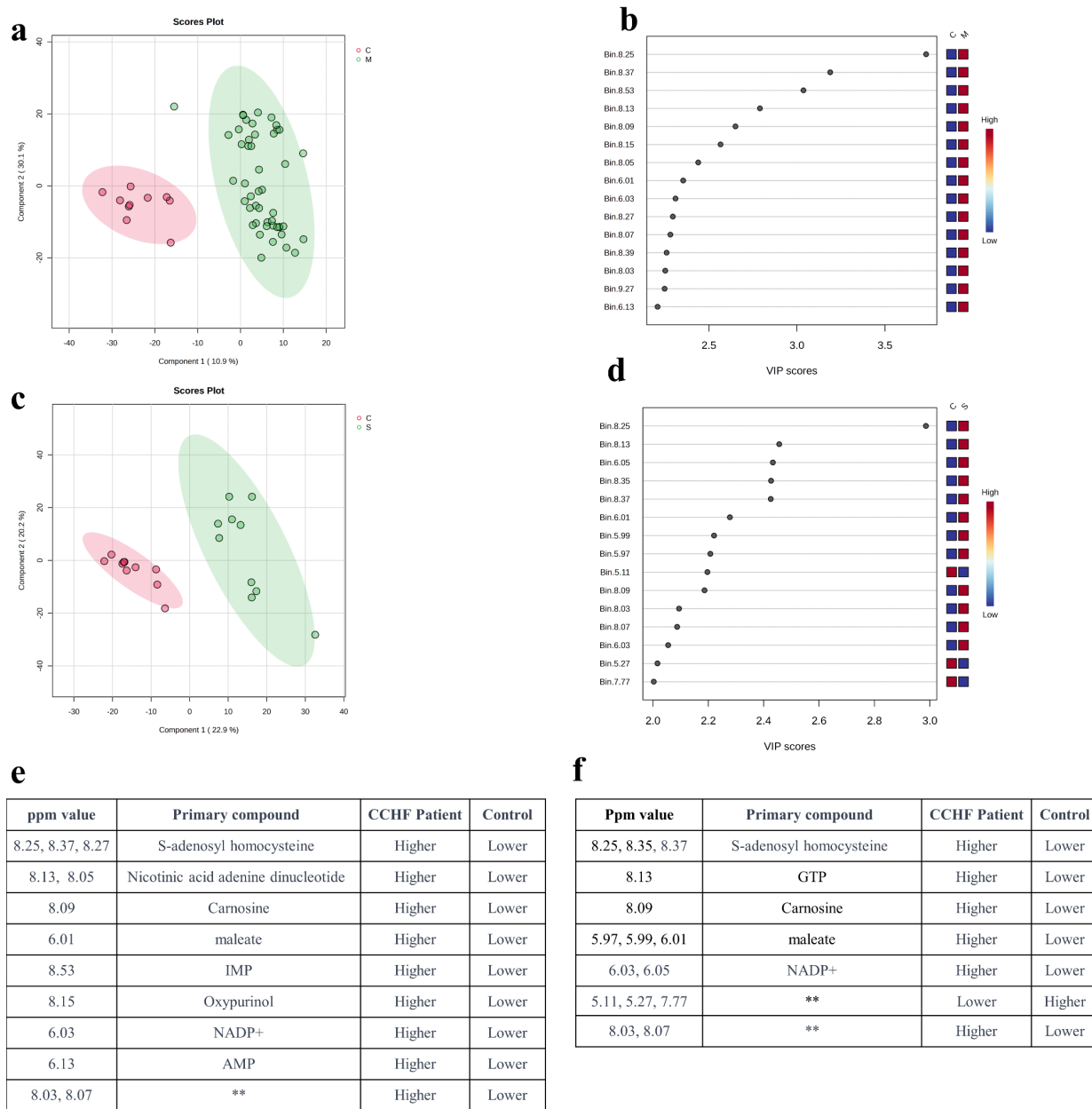


Figure 3: PLS-DA analysis of patient samples with moderate infection level for first two days with the control group and PLS-DA analysis of patient samples with severe infection level for first two days with the control group (S:severe, M: moderate, C:Control) a, partial Least Squares Discriminant Analysis score plot. Component 1: accuracy=0.983, ($R^2=0.821$, $Q^2=0.739$), component 2: accuracy=0.983, ($R^2=0.860$, $Q^2=0.790$), component 3: accuracy=0.983, ($R^2=0.954$, $Q^2=0.829$) b, Variable importance score plot in PLS-DA VIP Projection. c, partial Least Squares Discriminant Analysis score plot. Component 1: accuracy=0.950, ($R^2=0.857$, $Q^2=0.702$), component 2: accuracy=1, ($R^2=0.938$, $Q^2=0.797$), component 3: accuracy=1, ($R^2=0.982$, $Q^2=0.824$) d, Variable importance score plot in PLS-DA VIP Projection. e, corresponding compounds in detected increases on the spectra. f, corresponding compounds in detected increases on the spectra.

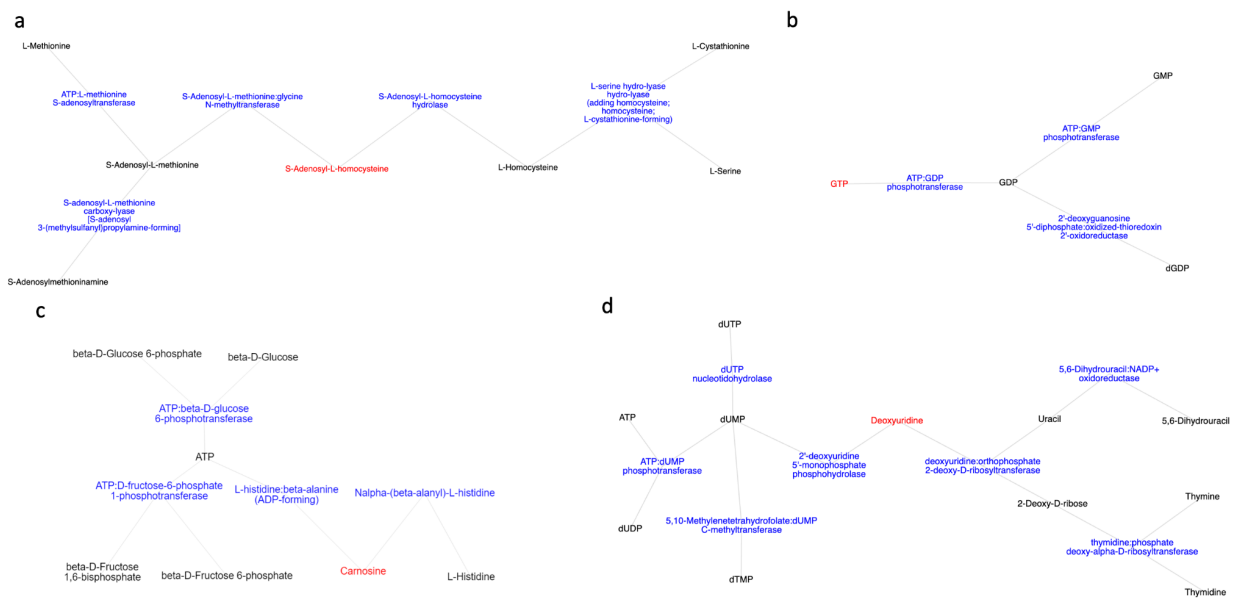


Figure 4: Main metabolic pathways of metabolites detected by metabolomics approach a. S-Adenosyl-L-homocysteine and nearest neighbor in Cysteine and methionine metabolism b. GTP and nearest neighbor in Purine metabolism c. Carnosine and nearest neighbor in Histidine metabolism d. Deoxyuridine and nearest neighbor in Pyrimidine metabolism